IOP Conf. Series: Materials Science and Engineering **188** (2017) 012038 doi:10.1088/1757-899X/188/1/012038

Different heat treatment of CeO_2 nanoparticle composited with ZnO to enhance photocatalytic performance

A Taufik[1,2], H Shabrany[1,2] and R Saleh[1,2]

[1]Department of Physics, Faculty of Mathematics and Natural Sciences Universitas Indonesia, Kampus UI Depok, Depok 16424, Indonesia
[2]Integrated Laboratory of Energy and Environment, Faculty of Mathematics and Natural Sciences Universitas Indonesia, Kampus UI Depok, Depok 16424, Indonesia

Corresponding author's e-mail: rosari.saleh@gmail.com

Abstract. In this study, ZnO/CeO_2 nanocomposites were prepared with four variations of the molar ratio of ZnO to CeO_2 nanoparticles. Both ZnO and CeO_2 nanoparticles were synthesized using the sol-gel method at low temperature, followed by different heat treatments for CeO_2 nanoparticles. Thermal phase transformation studies of the CeO_2 nanoparticles were observed at annealing temperatures of 400-800°C. The complete crystalline structure of CeO_2 nanoparticles was obtained at an annealing temperature of 800°C. The structural and optical properties of all samples were observed using several characterization techniques, such as X-ray diffraction (XRD), ultraviolet-visible diffuse reflectance spectroscopy, and Brunauer, Emmett, and Teller (BET) surface area analysis. The structural characterization results revealed that the prepared CeO_2 nanoparticles were quite crystalline, with a cubic structure. The photocatalytic activities of all samples were tested under visible irradiation. The obtained results showed that ZnO/CeO_2 nanocomposites with a molar ratio 1:0.3 exhibited the highest photocatalytic activity. Further understanding of the role of primary active species underlying the reaction mechanism involved in photocatalytic activity were carried out in controlled experiments by adding several scavengers. The detailed mechanism and its correlation with the properties of ZnO/CeO_2 nanocomposites were discuss.

Keywords: CeO_2, ZnO, photocatalytic, methylene blue

1. Introduction

Photocatalytic semiconductors have been widely used in organic dye removal due to their good ability to degrade organic dye [1]. Among multiple semiconductors, zinc oxide (ZnO) is the favored photocatalyst due to its good photocatalytic activity, eco-friendliness and low cost [2-3]. However, the ZnO photocatalyst still has limitations due to the high rate of electron recombination and holes; moreover, it can only be activated using ultraviolet (UV) light irradiation [4].

To overcome these problems, combining a ZnO semiconductor with another semiconductor has proven to increase the photocatalytic activity [5-7]. Cerium (IV) oxide (CeO_2) is an n-type semiconductor that has been commonly used as a supporting photocatalyst to increase photocatalytic activity [8-9]. The coupled CeO_2 semiconductor with ZnO is able to inhibit the electron recombination and hole rate through the process of electron and hole transfer from one semiconductor to the others [10].

The photocatalytic process is also influenced by the crystal structure of the photocatalytic material. Some researchers have stated that the better the crystal structure the photocatalyst material produces,

the better the photocatalytic activity will be [11-12]. This is due to the increasing charge carrier mobility of the photocatalyst [13]. Therefore, in this research, the photocatalytic activity that results from merging a ZnO semiconductor with CeO_2 under irradiating UV light and visible light is tested. In addition, the influence of the crystallized CeO_2 is analyzed through variations in calcination from 400°C to 800°C.

2. Experimental details

Cerium sulfate pentahydrate ($CeSO_4.5H_2O$), zinc sulfate heptahydrate ($ZnSO_4.7H_2O$), sodium hydroxide (NaOH), ethanol, and water were used as the starting material without further purification. CeO_2 nanoparticles were synthesized using the sol-gel method. Typically, $CeSO_4.5H_2O$ were dissolved into the water using a magnetic stirrer. Then, NaOH solution was added to the $CeSO_4.5H_2O$ solution. Next, the solution was heated to 80°C for 4 h. After that, the precipitates were separated from the solution using the centrifugation method. The precipitates were dried under vacuum condition, and finally, the dried sample was calcinated at temperatures of 400°C, 600°C, and 800°C.

ZnO/CeO_2 nanocomposites were synthesized using the sol-gel method. Typically, $ZnSO_4.7H_2O$ was dissolved in water using a magnetic stirrer, then NaOH solution was added dropwise into $ZnSO_4.7H_2O$ solution. Following this, the solution was heated to 80°C. After reaching a temperature of 80°C, the CeO_2 nanoparticles were dispersed in water using an ultrasonic bath for 30 min; dispersed CeO_2 nanoparticles were then added to the solution. The solution was stirred for 2 h. After the mixing process, the precipitates were separated using a centrifuge and washed using ethanol and water several times. The precipitates were aged overnight and then dried at a temperature of 100°C for 1 h under vacuum conditions.All samples were characterized using X-ray diffraction (XRD; Rigaku Miniflex 600), Brunauer, Emmett, and Teller (BET) surface area analysis (Quantachrome 2000), and UV-visible (UV-vis) diffuse reflectance spectroscopy (Shimadzu spectrophotometer).

The photocatalytic activity was tested under visible light irradiation with methylene blue as a model of organic pollutant. Typically, 0.3 g of the photocatalyst was dispersed in a 100 mL glass beaker containing 20 mg/L of methylene blue solution for 30 min under dark conditions to reach adsorption and desorption equilibrium. Following this, the samples were irradiated using visible light for 120 min. At 15-min intervals, the methylene blue solution was taken and analyze using UV-Vis spectroscopy. The methylene blue degradation was calculated based on the following equation (1) bellow:

$$\text{Degradation} = \frac{C_t}{C_0} \tag{1}$$

where C_0 is the methylene blue concentration before the photocatalytic process (mg/L) and C_t is the concentration of methylene blue for every 15-min span of data retrieval (mg/L).

In the photocatalytic activity experiment, the influence of additional scavengers was also analyzed; this analysis functioned to detect the species with the greatest roles in the photocatalytic activity. The scavenger used included sodium sulfate as an electron scavenger, ammonium oxalate as a hole scavenger, and tert-butyl alcohol as a hydroxyl radical scavenger.

3. Results and discussion

Figure 1(a) shows the methylene blue degradation using the CeO_2 photocatalyst with different annealing temperatures. The results show that CeO_2 nanoparticles with an annealing temperature of 800°C exhibited the best photocatalytic performance under visible light irradiation. The methylene blue degradation rate was analyzed using the pseudo–first order equation, as seen in figure 1(b); the results showed that the methylene blue degradation rate using CeO_2 photocatalyst before the annealing process was 0.00636 min^{-1}, and with the increasing of the annealing temperature to 400°C, 600°C, and 800°C, the degradation rate of methylene blue increased to 0.00719 min^{-1}, 0.00855 min^{-1}, and 0.00939 min^{-1},

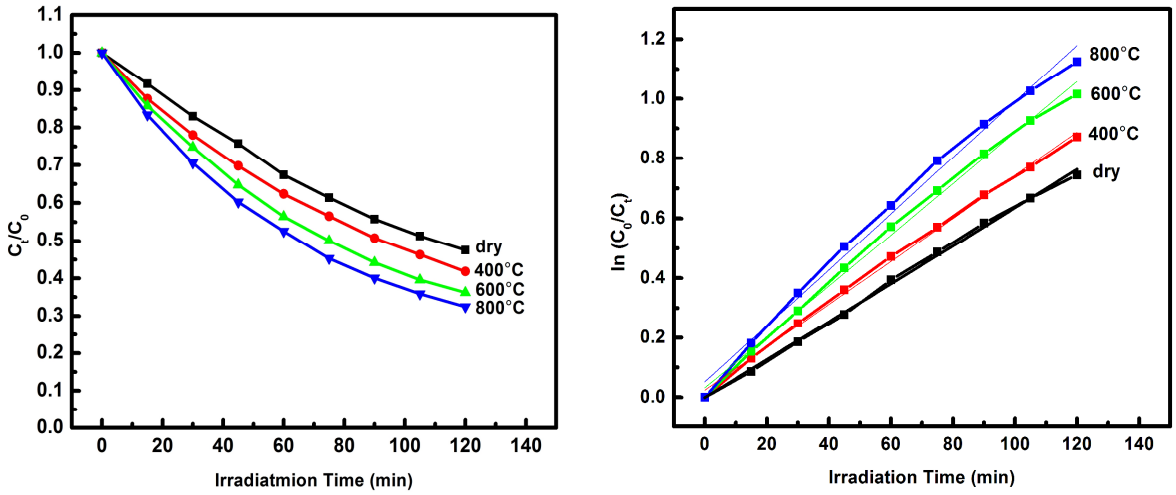

(a) (b)

Figure 1. (a) Photocatalytic and (b) linear plot ln (C_0/C_t) vs time of CeO_2 nanoparticles with different annealing temperatures

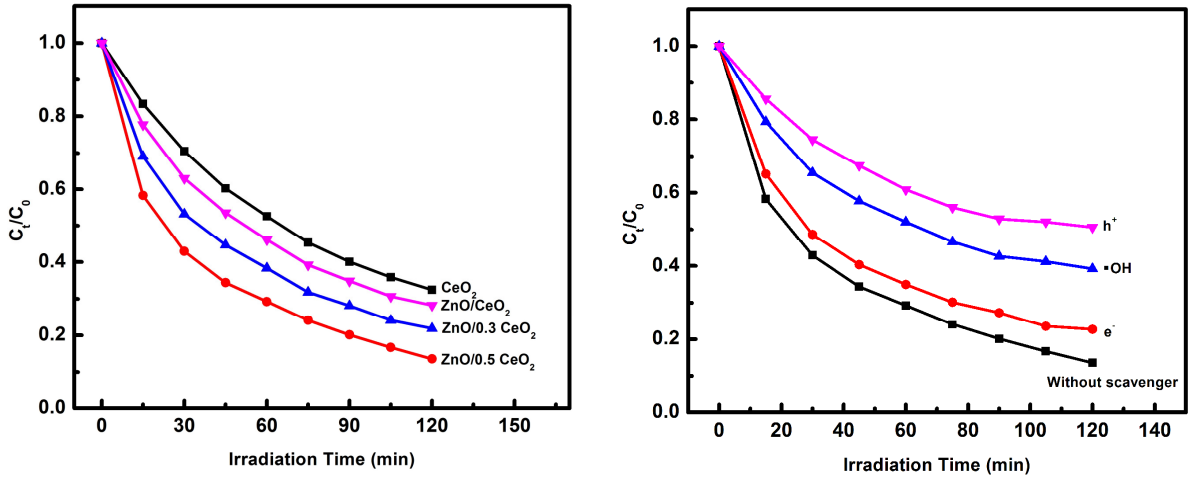

(a) (b)

Figure 2. (a) Photocatalytic activity of ZnO/CeO_2 nanocomposites with different molar ratio and (b) Effect of scavenger addition on photocatalytic performance of ZnO/CeO_2 nanocomposites.

respectively. Therefore, the CeO_2 nanoparticles with an annealing temperature of 800°C were used as composite material with the ZnO semiconductor.

The methylene blue degradation efficiency of the ZnO/CeO_2 (1:0.3, 1:0.5, 1:1) nanocomposite samples under visible light irradiation are shown in figure 2(a). The findings show that the usage of ZnO/CeO_2 nanocomposite with a molar ratio 1:0.5 resulted in the best degradation ability under visible light irradiation.

Figure 2(b) shows the influence of scavenger addition to the photocatalytic activity of the ZnO/CeO_2 sample with molar variation of 1:0.5 under visible light irradiation. The results show that the addition of scavengers decreased the photocatalytic activity of the sample. This occurred due to the scavenger addition captured electron, hole, and OH radicals, which played a role in the photocatalytic process in association with each scavenger used. It can be seen that the addition of ammonium oxalate resulted in

the lowest photocatalytic activity under visible light irradiation. This finding indicates that the hole was the most active species in terms of the degradation of methylene blue.

Figure 3(a) shows the XRD measurement of CeO_2 nanoparticles with different annealing temperatures. The XRD result showed that the CeO_2 nanoparticles had a cubic structure with planes of diffraction of (111), (200), (220), (311), (222), (400), (331), (420), and (422). It can be seen that with an increasing annealing temperature, the diffraction pattern CeO_2 became sharper. Thus, improvement was observed in the crystallized sample. The grain size and lattice parameter of the CeO_2 nanoparticles for all annealing temperatures were analyzed using the Debye–Scherrer equation [14] and Rietveld refinement model. The obtained result is shown in table 1. The grain size of the sample increased from 2 nm to 25 nm.

Figure 3(b) shows the XRD curve of the ZnO/CeO_2 nanocomposites with molar ratios of 1:0.3, 1:0.5, and 1:1. For comparison, the XRD curves of ZnO and CeO_2 are also shown in the figure. It can be seen that the existence of the hexagonal wurtzite phase of ZnO and the cubic phase of CeO_2 could be detected from the XRD measurement. The ZnO structures were successfully detected at $2\theta = 31°$, 34°, and 36°, which indicates the existence of planes (100), (002), and (101), while $2\theta = 28°$, 32°, 47°, 56°, and 59° indicated the existence of planes (111), (200), (220), (311), (222), and (400), corresponding to the cubic phase of CeO_2. It can be observed that the diffraction peak of the cubic phase of CeO_2 increased with greater CeO_2 content in the ZnO/CeO_2 nanocomposite. The lattice parameter and grain size are also shown in table 1. The results show that the lattice parameters of ZnO and CeO_2 did not change significantly when they were formed into a nanocomposite. However, the measurement value grain size of ZnO decreased along with the addition of molar CeO_2.

The measurement test of surface area of all samples is shown in table 1. The result obtained shows that along with the increase of annealing temperature, the value of surface area of CeO_2 sample decreased from 76 m^2/g until 13 m^2/g. The decrease of surface area value when annealing temperature was improved caused by the increase of grain size measurement of CeO_2 sample. The value of surface area sample increase from 23 m^2/g until 105 m^2/g when it was formed into ZnO/CeO_2 nanocomposite.

The UV-Vis absorbance of ZnO/CeO_2 with molar ratios of 1:0.3, 1:0.5, and 1:1 are shown in figure 4. The figure demonstrates the light absorbance ability of samples from wavelengths of 200-800 nm.

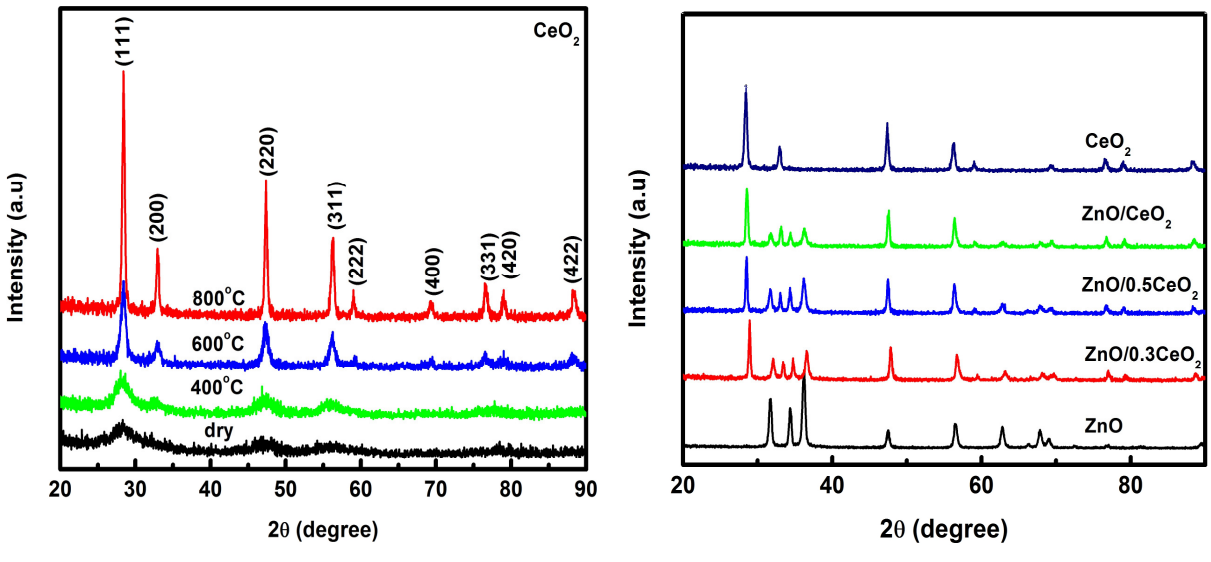

Figure 3. (a) XRD spectra of CeO_2 nanoparticles and (b) ZnO/CeO_2 nanocomposites with different molar ratio.

Table 1. Lattice parameter, grain size and BET surface area of CeO_2 nanoparticles with different annealing temperatures and ZnO/CeO_2 nanocomposites with different molar ratio.

Sample	Lattice Parameter (Å)			Grain Size (nm)		Surface Area (m^2/g)
	CeO_2	ZnO		CeO_2	ZnO	
	a	b	a			
dry	5.397	-	-	2	-	76
CeO_2 400°C	5.416	-	-	4	-	57
CeO_2 600°C	5.419	-	-	9	-	34
CeO_2 800°C	5.421	-	-	25	-	13
ZnO/0.3 CeO_2	5.422	3.259	5.220	23	25	105
ZnO/0.5 CeO_2	5.414	3.253	5.216	21	20	45
ZnO/CeO_2	5.413	3.253	5.212	21	19	23

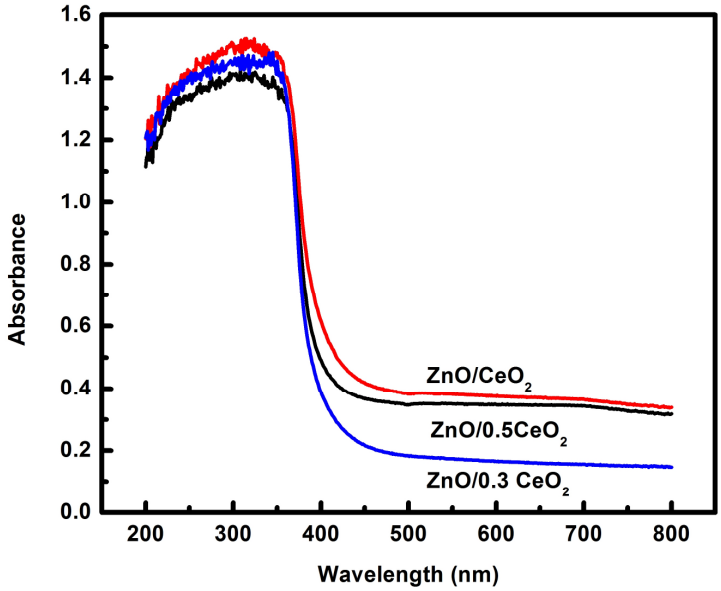

Figure 4. UV Vis absorbance spectra of ZnO/CeO_2 nanocomposites.

The results showed that the light adsorption ability of ZnO/CeO_2 nanocomposite in the visible light range increased with greater CeO_2 loading. The band gap energy of all the nanocomposite samples was calculated with the Kubelka–Munk equation [15]. The results showed that the band gap energy of the sample exhibited a slight decrease with increased CeO_2 loading. This indicates that the ZnO/CeO_2 nanocomposite sample may be activated under visible light irradiation.

Based on the photocatalytic measurement, the photocatalytic activity of the CeO_2 sample increased with the addition of annealing temperature. This was because the higher crystallinity of the sample plays an important role in the photocatalytic process. As could be seen in the XRD measurement, the annealing temperature of 800°C resulted in the highest crystallization. With the higher crystallinity of the sample, the mobility of the charge carrier was also improved, and the photocatalytic activity could be enhanced [13]. In this case, the surface area of the samples did not have a significant influence on the photocatalytic process.

The formation of ZnO/CeO_2 nanocomposites can increase the methylene blue degradation ability due to the charge transfer from each band structure of ZnO and CeO_2. Some studies showed that the conduction and valence bands of the ZnO and CeO_2 positions allow the electron and holes to transfer from one semiconductor to the other. The charge transfer process can inhibit the recombination of electrons and holes; thus, the photocatalytic activity increases [10].

4. Conclusions

CeO_2 nanoparticles with an annealing temperature of 800°C showed the highest crystallinity and photocatalytic performance. The surface area value did not have much influence on the photocatalytic process. The formation of ZnO/CeO_2 nanocomposites is able to increase the photocatalytic activity capacity under the irradiating visible light caused by recombination electron and hole inhibition.

References

[1] Chong R, Cheng X, Wang B, Li D, Chang Z and Zhang L 2016 *Int. J. Hydrogen Energy* **41** 2575-82
[2] Bao Y, Wang C and Ma J Z 2016 *Mater. Des.* **101** 7-15
[3] Zhu C, Lu B, Su Q, Xie E and Lan W 2012 *Nanoscale* **4** 3060-4
[4] Yin H, Yu K, Song C, Huang R and Zhu Z 2014 *ACS Appl. Mater. Interfaces* **6** 14851-60
[5] Shirzadi A and Ejhieh A N 2016 *J. Mol. Catal. A: Chem.* **411** 222-9
[6] Mageshwari K, Nataraj D, Pal T, Sathyamoorthy R and Park J 2015 *J. Alloys Compd.* **625** 362-70
[7] Kalpana K and Selvaraj V 2015 *Ceram. Int.* **41** 9671-9
[8] García M E C *et al.* 2014 *Mater. Sci. Eng.,* B **183** 78-85
[9] Lv Z, Zhong Q and Ou M 2016 *Appl. Surf. Sci.* **376** 91-6
[10] Lamba R, Umar A, Mehta S K and Kansal S K 2015 *J. Alloys Compd.* **620** 67-73
[11] Li D, Cheng X, Yu X and Xing Z 2015 *Chem. Eng. J.* **279** 994-1003
[12] Chong R, Cheng X, Wang B, Li D, Chang Z and Zhang L 2016 *Int. J. Hydrogen Energy* **41** 2575-82
[13] Zhang S, Gu X, Zhao Y and Qiang Y 2015 *Mater. Sci. Eng., B* **201** 57-65
[14] Srivastava S, Sinha R and Roy D 2004 *Aquat. Toxicol.* **66** 319-29
[15] Hapke B 1993 *Theory of Reflectance and Emittance Spectroscopy* (Cambridge: University Press)